POSITRON ANNIHILATION SPECTROSCOPY FOR THE CHARACTERIZATION OF DEFECTS IN GAMMA IRRADIATED Ca-DOPED $MgFe_2O_4$ AND MgO SAMPLES

PATRIC V LOBO

INTEGRATED M.Sc. PHYSICS

(10^{th} SEMESTER)

AM.AR.I5PHY11015

DEPARTMENT OF PHYSICS,

AMRITA UNIVERSITY, KERALA.

ACKNOWLEGMENT

I would like to express my sincere gratitude to all those who have helped me complete my project work. First of all, I thank my guide and mentor **Prof. P.M.G. Nambissan**, Professor-G, Applied Nuclear Physics Division (ANPD), Saha Institute of Nuclear Physics, Kolkata, for supervising and enlightening me with his lore on positron annihilation spectroscopy. I also acknowledge my instructor, **Prof. Narayan Kutty**, Head of the Department of Physics, Amrita, for letting me to do my final year project at Saha Institute of Nuclear Physics. I am grateful to the Director of SINP for granting me permission to work in the Applied Nuclear Physics Division. I have to mention the support and generosity of **Prof. Satyajit Saha,** Head of ANPD at SINP for arranging the necessary requirements. I like to speak my special thanks to **Mr. Kuntal Sarkhel**, **Mr.Pradipta Kumar Das** and **Mrs. Soma Roy** for aiding me in the laboratory and also to my co-worker **Mr. Vikrant Singh** from Amity University, Delhi, for his encouragement and hard work. Nevertheless, I thank all my teachers and friends for their ceaseless push and furtherance. Finally I thank my family for allowing me to travel so far away from home and recognizing my potential.

ABSTRACT

Positron annihilation spectroscopy is one of the many modern techniques used in analyzing defect sample. The results are accurate to a very good precision, taking into account the expenditures met with other techniques. The studies made on gamma irradiated undoped magnesium ferrite samples observed under different temperatures as well as gamma irradiated magnesium ferrite samples that are doped at different concentration with calcium and the inspection of magnesium oxide samples doped with calcium are elaborated in this report. The assay of gamma irradiated magnesium ferrite samples are compared with that of the pre-irradiated magnesium ferrite samples to find out the dominant changes. The data from nanocrystalline magnesium oxide samples (which I carried out) are compared with that of the previously obtained larger magnesium oxide report. The differences in lifetimes of positron seen from the above comparison lay open the change in atomic structures as one move to nanoscale, along with many other information such as the change in general properties of the materials and rate

of evolution of defects within the sample on reducing the particle size. These particles are under the presumption to be very beneficial in various fields where their functions are to be specific.

Chapter 1

POSITRON ANNIHILATION SPECTROSCOPY

Introduction

Positron annihilation spectroscopy is a relatively modern technique that is used in the study of materials, both solidified and powdered. As a part of my project, I am using this positron annihilation process to understand the structure and the corresponding defects in several powdered nanomaterials. It is being recognized as a powerful method to extract information regarding a sample, such as the types of defects and their densities, since it measure changes for low defect concentration where the other method fail. It is also a non destructive process. The defects in sample alter several major intrinsic properties of the sample and hence its studies are important. Therefore the PAS technique is very much reliable in the future.

Theory

Positrons are the result of positive beta decay, and are the antiparticles of electrons. Positrons are thus emitted from various sources such as ^{58}Co, ^{22}Na, ^{64}Cu etc. Positrons from the source, on entering the sample or solid attain thermal energy due to phonon interaction, collisions and electron hole pair excitations. Such positrons annihilate with electrons within the sample. Such reactions lead to the emission of two gamma rays in almost opposite directions.

The time delay between the production of positron and detection of annihilation gamma rays gives the lifetime of positrons. In my experiments, two photomultiplier tubes fitted with a scintillator each are used for measuring this time interval. From such lifetime data, the concentration of electrons in the sample is obtained. Also, two germanium detectors are used to obtain a spectrum concerning the energy of the two gamma rays. From this data, the electron momentum distribution is found.

Actually, there is one method to calculate the positron lifetime and two methods which depend on the conservation of momentum, during the positron-electron annihilation, to find out the electron momentum distribution within the sample. The lifetime spectrum is acquired by the study of rate of annihilation of positrons inside the sample, while we can get the momentum distribution of electrons within the sample using Doppler broadening spectrum or Angular correlation spectrum.

Lifetime Technique

As I mentioned above, positron lifetime spectrum is essential to determine the electron density in a sample. To obtain the lifetime of one positron we need to note down the time of production of the positron and the time of annihilation. The method of indication of the production of positron is explained later, in experimental detail, and the end of positron life is marked by the detection of the pair annihilation gamma rays.

First of all, we consider the annihilation rate of positrons to be similar to the exponential decay during radioactive emissions. Let us, for a start, assume a sample without defects. Let n_b be the number of positrons in a sample at an instant. Here the positrons are called bulk positrons. By our earlier assumption:

$$dn_b/dt = -\lambda n_b$$

Here λ is the rate of annihilation of positrons.

The rate of annihilation of positrons depends on the density of electrons around the point of annihilation:

$\lambda = \pi r_0^2 c\, \xi(r)\, n_e$; where r_0 is classical electro radius, c the velocity of light and $\xi(r)$ is electron density enhancement factor which accounts for the increase in electron due to coulomb attraction by positrons.

However, a perfectly aligned crystal lattice is not practical. The presence of defects alters the properties of the sample very much, especially that of nano-crystals. There are defects that traps a positron, for example, the presence of vacancy in crystal lattice reduce the electron density at that particular point and hence positrons entering such a lattice have longer life. As the electron density at a defect is different than of the regular arrangement, the positron lifetimes also varies much, depending on the type of defect. If n_d is the number of positrons in defects at a time t then the reduction rate of bulk positrons is:

$dn_b/dt = -\lambda n_b - k_d n_b$; where k_d is rate of transfer of positrons from bulk to these traps. The solution is $n_b = N_0 \exp(-\lambda_1 t)$. Here $\lambda_1 = \lambda_b + k_d$. In terms of lifetime components the equation becomes:

$$1/\tau_1 = 1/\tau_b + k_d$$

The positrons in defects get annihilated at a rate λ_d. Reduction rate of such positrons is :

$$dn_d/dt = -\lambda_d n_d + k_d n_b$$

Doing the appropriate integration and applying initial condition that $n_d=0$ at t=0, we get

$n_d = -k_d/(\lambda_1-\lambda_d) \exp(-\lambda_1 t) + k_d/(\lambda_1-\lambda_d) \exp(-\lambda_d t)$

In our experiments it is arranged for the N_0 to be 1. Hence the positron is in either n_b or n_d. The problem with the above assumption is that they represent 2 state trapping model; which suggest that only one type of defect exists in the sample. If there are 'm' numbers of defects, m-state trapping model is to be used.

In addition to defects, it is possible for another lifetime reading, where the positron form a bound state with an electron known as the positronium. However, they do not last long in this state, and annihilate with each other. Positroniums are less common in materials of high electron density, but the intergranular regions in nanomaterials tend to the formation of positrons by a small fraction. As the size of crystallites reduces, more space is produced for the positronium formation. Hence, the positronium intensity increases with the reduction in size of the nanoparticles. But also, instead of forming positronium in such interstitials, such sites may act as defects and get annihilated directly. In case of large volume defect samples, the probability of forming a positronium is high. Therefore, assuming the defect to be a sphere, one can calculate the average size of these defects by the equation:

$T_3 = 0.5/[1-(R/R_0)+(1/2\pi)\sin(2\pi R/R_0)]$, where $R_0=R+\Delta R$, ΔR being empirical electron layer thickness equal to 1.66 Armstrong. Along with this the free volume fraction is also calculated by the equation $f = AV_fI_3$, A is a constant and V_f is the free volume.

The two ground states of positronium are para-positronium, where the positron and electron have antiparallel spins, and ortho-positronium, where the spins are parallel. Therefore para-positronium is a spin singlet state and ortho-positronium is a triplet state. The intensity of positronium in the sample is small, except in

a few cases as that of polymers etc., where even the intensity of para-positronium (which is about one-third of that of ortho-positronium) is not neglected. Having opposite spins para-positronium annihilates the fastest, having a lifetime about 125ps, emitting even number of gamma rays. Ortho-positroniums have a lifetime upto 140ns in vacuum and emit odd number of gamma rays. But in material medium it captures an electron from the surroundings and annihilates within a few nanoseconds and emits a pair of gamma rays.

The above mentioned three lifetimes are the common lifetimes obtained during analysis. Further lifetimes may be obtained depending on the sample used. For example, if the sample contains nanorod cavities one may expect a total of four lifetimes owing to the large lifetime of positronium in these cavities.

Doppler Broadening Technique

Ideally, two gamma rays of equal energies are emitted in opposite directions after pair annihilation. But realistically it won't necessarily happen. This is because of imparted momentum by the annihilating electron. Gamma emitted in the same direction as that of electron will have higher energy, but the total energy remains constant. Hence one photon has 0.511+ΔE MeV and the other have 0.511-ΔE MeV. This is called Doppler shift. If p_L is the longitudinal momentum component of electron, $\Delta E = p_L c/2$.

The core electrons contribute more to the broadening in the p_L vs ΔE spectrum, since they have higher momentum. Positrons will have only thermal energy before annihilation and hence by measuring ΔE the momentum distribution of electron can be found out.

Coincidence Doppler broadening spectroscopy (CDBS) is enhanced method of monitoring broadening effects due to the core electrons. Two high-pure germanium detectors are placed to capture the two gamma rays and to gate the signals to a multi channel analyzer to obtain a coincidence spectra. A spectrum is produced with E_1+E_2 on the x-axis and E_1-E_2 on the y-axis. A projection of the events within a central window $1.022 \pm 2Emax$ along the direction parallel to E_1-E_2 axis will give a Doppler broadened energy distribution free of resolution and background. From this projection the elemental environment can be studied.

Angular Correlation Technique

The orbital electron can have its linear momentum in any direction and hence the emitted gamma rays may not be exactly opposite to each other but scattered by a small angle. Gathering large data about this angle of scattering, the information regarding electron momentum can be found using this method, and even more precise than the Doppler broadening technique. However, I have not conducted it in my lab due to the lack of instruments.

The above mentioned lifetime, CDBS and angular correlation spectroscopy together form the positron annihilation spectroscopy (PAS). PAS have several advantages over other methods like XRD and TEM, giving information on atomic level and being a non-destructive process. Slow positrons have shown depth sensitivity. It has found many applications, especially in the research of material physics and condensed matter. It is used for medical imaging and other imaging systems like positron emission topography. And also, since new made nanomaterials are changing the world with their peculiarities the study of such materials is also growing important. PAS gives a more accurate detail of the material. PAS is widely used for the study of formation and migration of vacancies. The energy associated with the formation of a vacancy is calculated with acceptable efficiency. It is not as accurate as de Haas – van Alphen measurement technique in determining electronic structure in solids such as pure metals and ordered alloys, but de Haas – van Alphen measurement technique fails in randomly disordered alloys, because the mean free path of electron is lower than required for such measurements. A good account on the Fermi surfaces in metals, alloys and compounds can be attained using PAS (through angular correlation).

The disturbance on defect free electronic system under observation is a disadvantage to the method as the precision in electronic structure study is reduced, though momentum distribution studies are not much affected.

Another disadvantage is that positrons may prefer one element over other in complex compounds. Also, because the electron density around a positron is higher the veracity in finding information about structures of samples other than simple metals is hard, as this enhancement of electron density is hard to come by for such samples. One other major con is that the positrons being positively charged cannot enter an oxygen deficient site since such a site is comparatively positive, oxygen being electro-negative. Hence analyses on several oxides are limited, that is, only the cations can be replaced.

Chapter 2

EXPERIMENTAL DETAILS

Let me introduce the necessities for the positron annihilation spectroscopy. There is a source for emitting positrons and while experimentation the source is placed in middle of the sample. If the sample is a solid, the source is kept between the sample plates, while, if it is a powdered sample the source is encompassed inside at the centre of the sample. There are two scintillation detectors fitted with a photomultiplier tube each, which are to be kept opposite facing each other around the sample. There are also two high pure germanium detectors kept facing each other perpendicular to the imaginary axis connecting the two scintillation detectors. For all these detectors are provided the sufficient power supply for operation. Proper care must be given that the rate of photons falling must be low enough that the detectors are able to distinguish between each pulse, at the same time the rates must be high enough that sufficient data is acquired within the preferred date. The sample is kept in the junction of these four detectors, either inside a test tube – if it is a powdered sample or held by a holder clip – if the sample is solid. The powdered sample kept in tube has to be ceaselessly evacuated using a vacuum pump to remove the air in between the granules.

Background radiations are everywhere in the world- from the walls and underground etc. Apart from the radiation due to source, background radiations are also detected. During the analysis of the spectra, we have to separate these background radiations from the original.

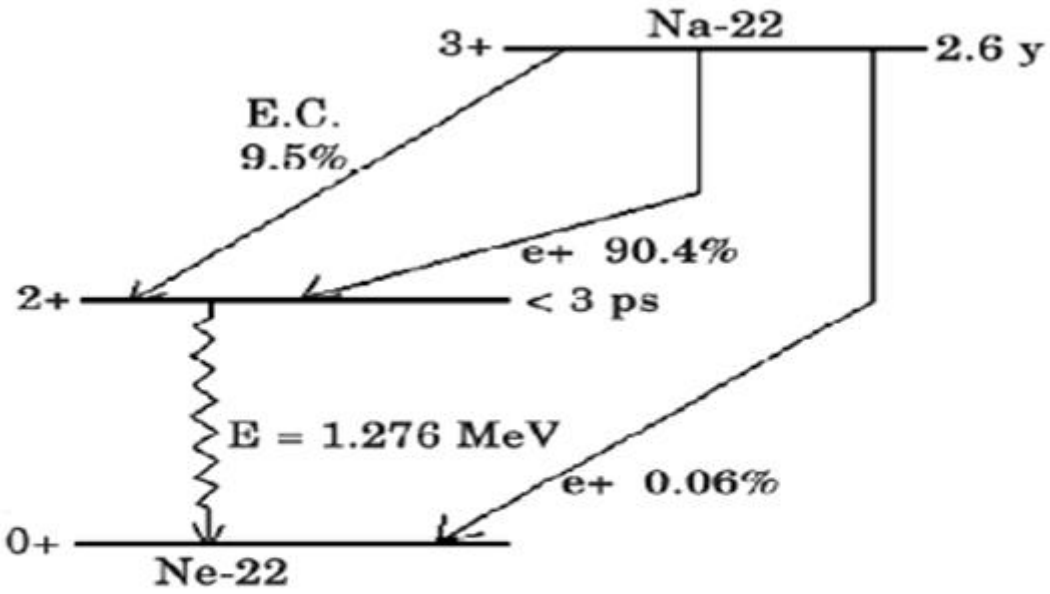

Figure2.1. Emission of the ^{22}Na source

The source I used in my experiments is ^{22}Na, which emits a gamma ray of energy 1.276MeV almost at the same instant as the emission of positron. Hence this gamma ray points to the time of creation of positron and is called the birth gamma ray while the annihilation gamma rays denotes the death of the positron, known as death gamma ray. The time interval between detection of these gamma rays is the positron lifetime. The positron emitted from the source enters the sample and annihilates within the sample. The gamma rays due to annihilation can be in any direction. Only those detected by the detectors are counted.

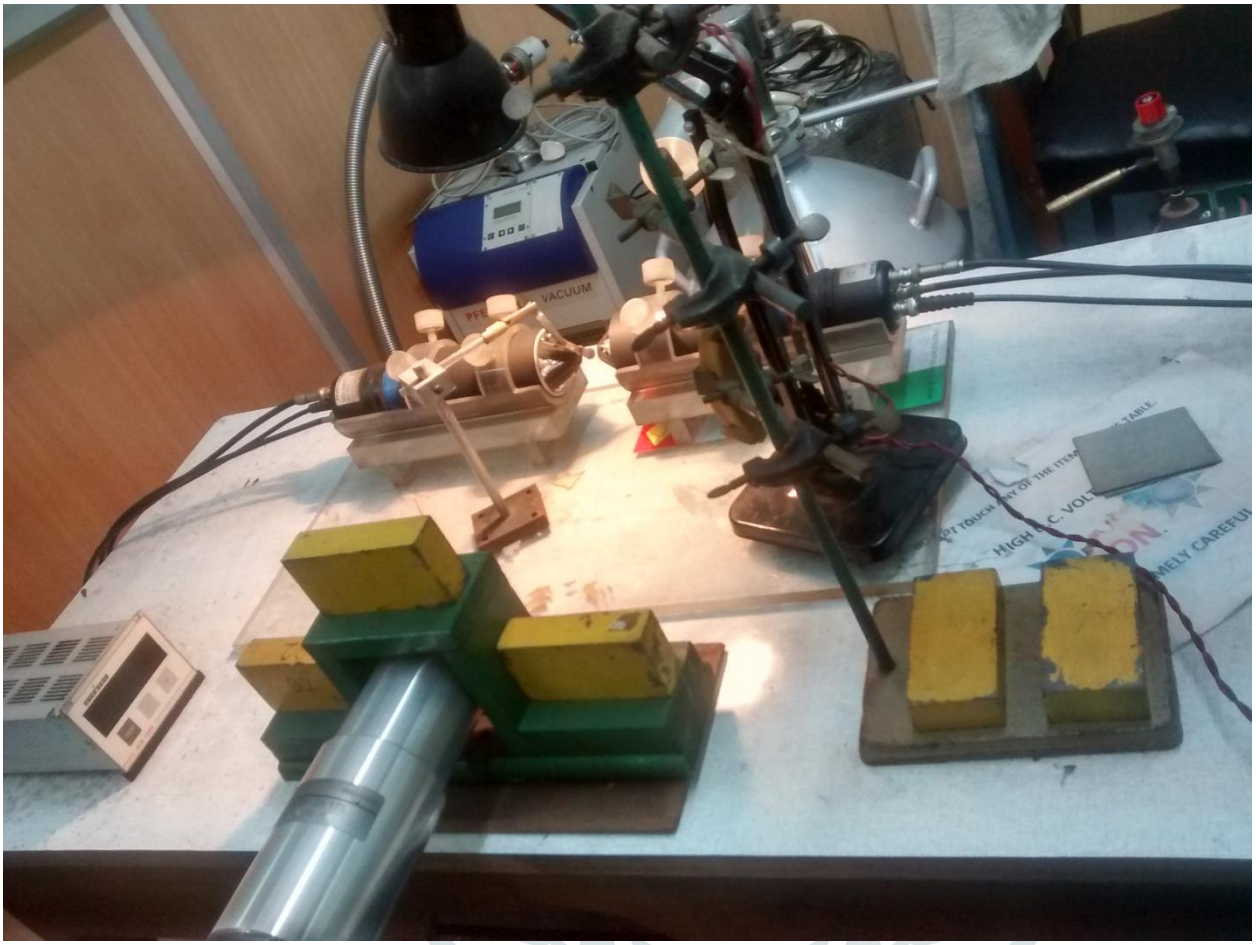

Figure2.2. All the four detectors

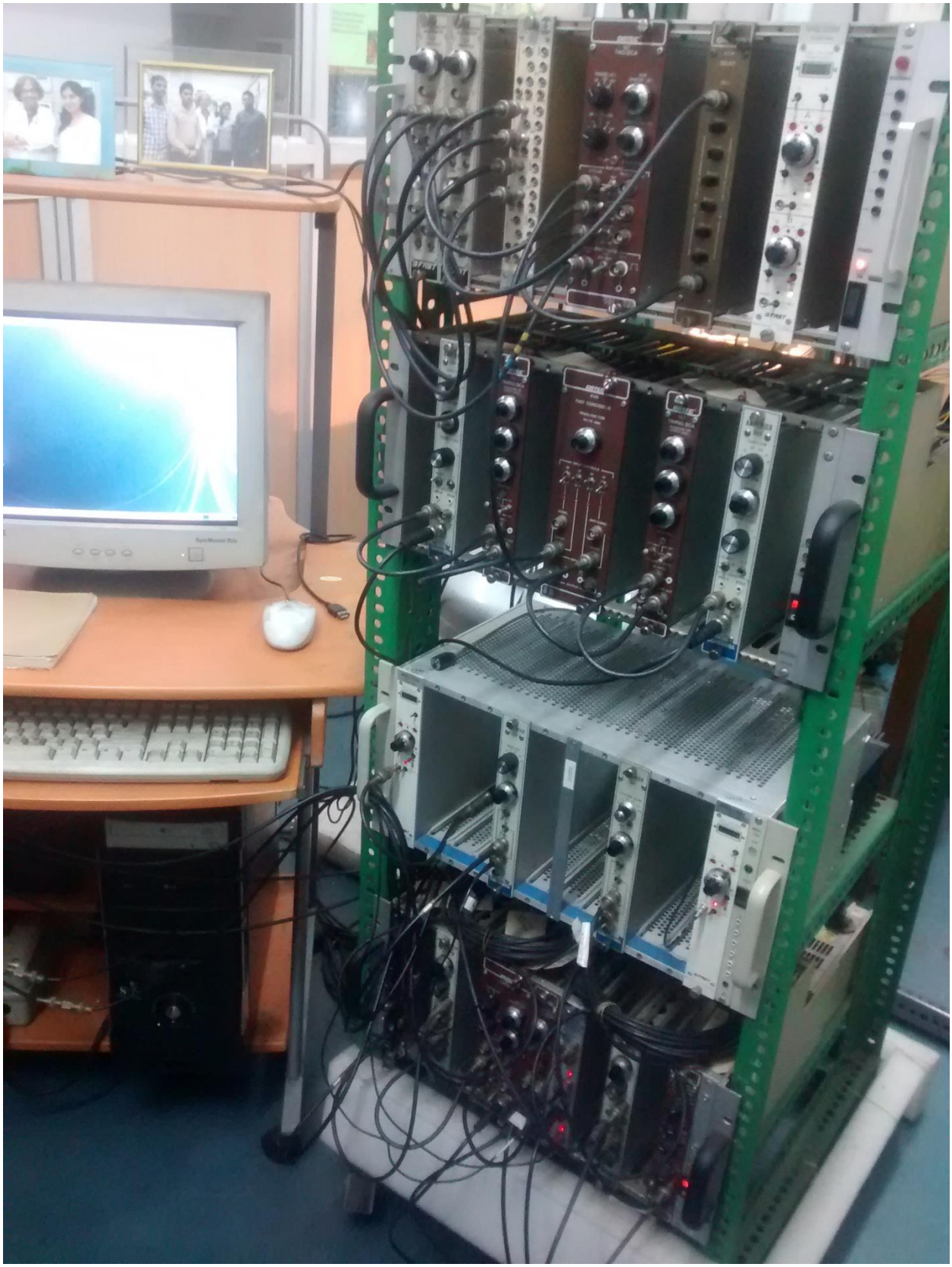

Figure2.3. Instruments

Lifetime Measurements

Lifetime measurements are done using the scintillation detectors, whose resolution are not as good as the HPGe detectors but nevertheless adequate for data analysis.

Scintillators are materials in which the electron excites and de-excites very fast. The falling high energy gamma rays imparts its energy to a lot no of electrons and on sudden de-excitation emit large number of low energy photons. These photons fall on with other material, which easily undergoes photoelectric effect and emit electrons. Each gamma ray could have emitted only one electron from an atom and that is why we split them to

subsequent photons, and using a scintillator eliminates the time lag of the event. There may be scattering of the photons within the scintillator which affects the birth or death signal, so we cover the scintillator with a reflecting surface, with the reflecting surface coming on the inside to prevent the escape of these photons outside.

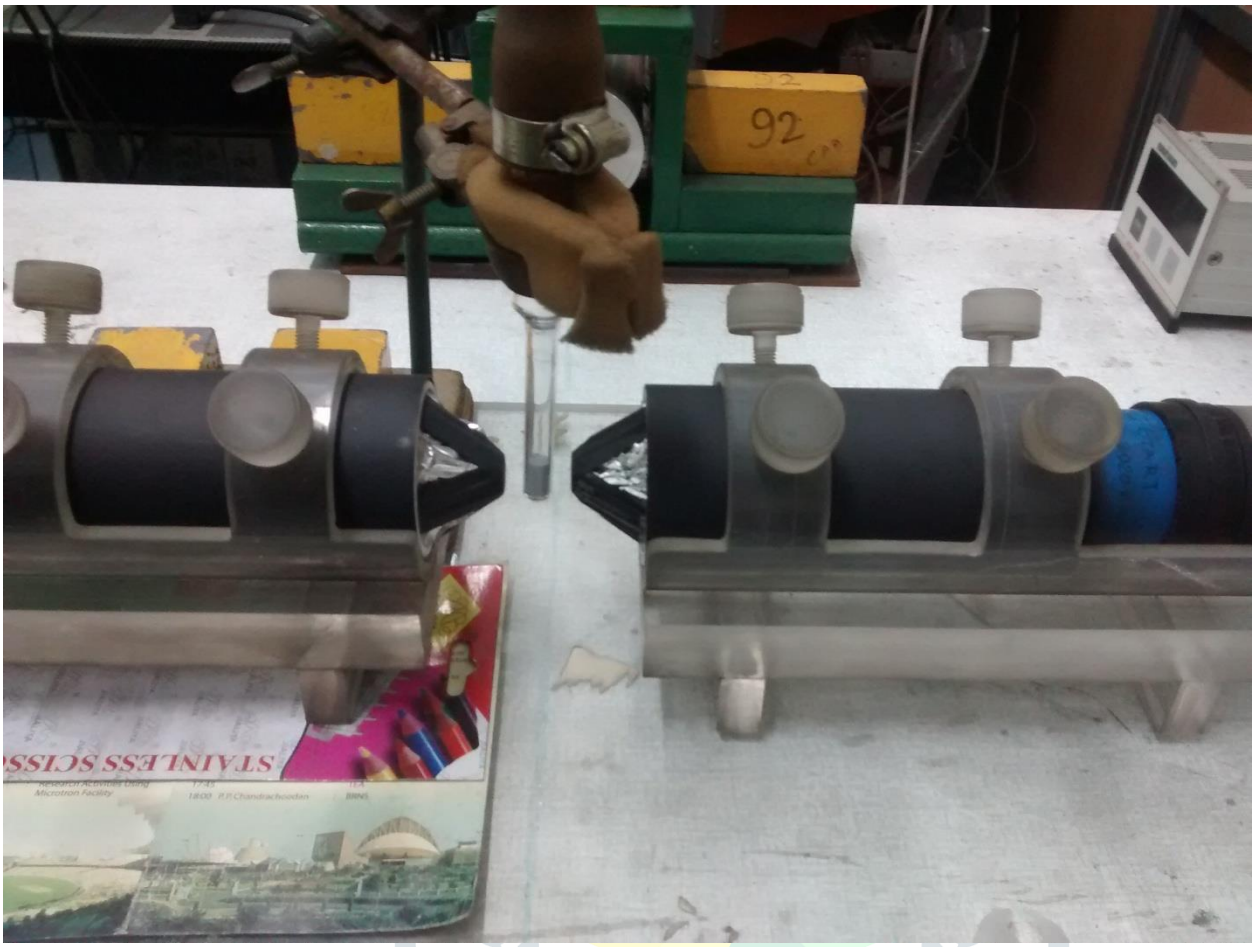

Figure2.4. Scintillation detectors

Figure2.5. Photomultiplier Tubes

PMTs are coupled to the scintillators. More amounts of electrons are to be produced, because on increasing the current in ample quantity we produce sufficient voltage enough for the signal that we use for birth and death gamma rays. The substance that undergoes photoelectric effect was called as dynodes. Since more electrons leave dynodes than the electrons arriving, they have a net positive charge. Hence a second signal can be acquired from dynodes, first being collected from anodes. The detectors may detect wrong vibrations like

detecting a death gamma ray first and then a birth gamma ray. It is for this reason we produce two signals, one from anode and the other from dynode.

The anode signals are used to calculate time interval precisely with the help of TAC. There may also problems such that either one of the death or birth gamma ray or both of them may produce low signals, the results of which are erroneous. In order to minimize such errors we use constant fraction discriminators (CFD). There is a capacitor inside the TAC which starts charging when any signal reaches the TAC first and stops at the next signal. The voltage across the charging capacitor is exponential with time, but, there is a region of the exponential graph where the voltage varies linearly with time. This is the area of functioning of our capacitor. Between the start and stop signal, the capacitor develops a specific voltage across it, corresponding to the time interval, which is forwarded towards the MCA.

The incoming signals from dynodes are received through two single channel analyzers (SCA). The lower and upper threshold of the SCAs can be adjusted so that one SCA is to record the birth gamma ray while the other records the death gamma ray. The two SCAs are ANDed into the fast coincidence instrument. If the signal voltages are adequate enough to be perceived by the SCAs and reach the fast coincidence instrument within a preferred interval of time- the resolution time – then we can be quiet sure that it is a genuine radiation rather than a faulty one. The output this fast coincidence is used to strobe the TAC, to which the signals from anodes reach.

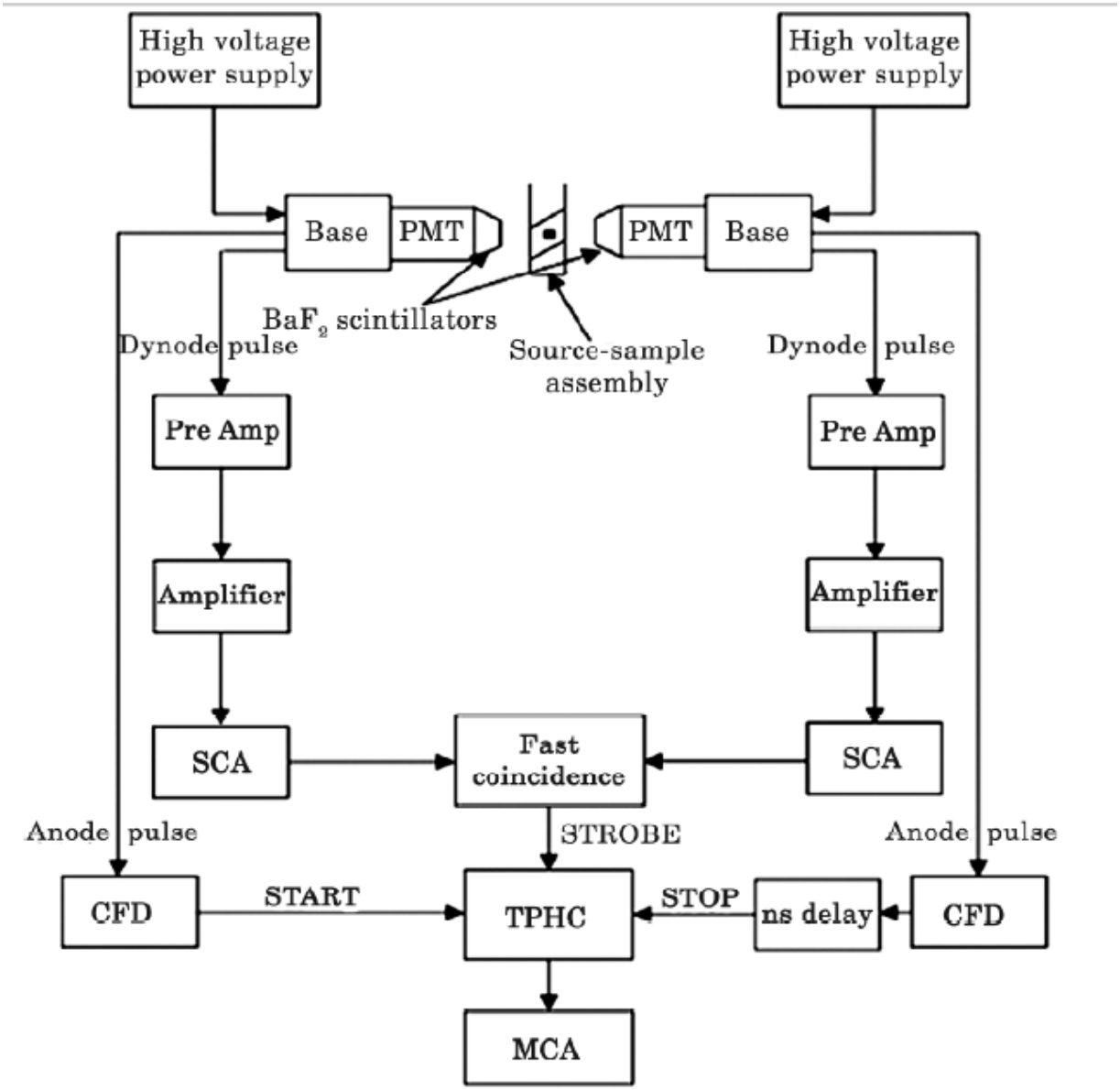

Figure2.6. Block Diagram of Lifetime analysis instruments

The lifetime of positrons is represented as a sum of exponential components:

$N(t) = \sum_1^n I(i) \exp(-\lambda(i)t)$ where the annihilation rates $\lambda(i)=1/\tau_i$, and the intensities I(i) can be found out by computational procedures. Here n is the number of possible lifetimes; i.e. if there are k defects, n=k+1. Also, finding the mean positron lifetime helps in discovering the evolution of the defects.

Before analyzing a sample using a ^{22}Na source, the resolution of the detector is found out by using a ^{60}Co source. The resolution is noted in terms of FWHM.

Data Analysis

The spectrum is obtained in gamma acquisition software, where a peak is obtained with an exponential curve on its right hand. The graph contains several channels in the x-axis and counts in the y-axis. In our case the channel number was 2048. The difference between the first and last channel is adjusted by changing the range in TAC. The difference represents the range of time, which is divided equally among the 2048 channels. Thus increasing the range decreases the precision in lifetime. This spectrum will not work properly at the extreme. Hence we apply delay to shift the spectrum to the proper functioning region of the spectrum. The obtained spectrum is to be stripped of its longest exponential term first and the corresponding intensity is to be found. The remaining spectrum has to be stripped of its longest exponential term. Hence a second lifetime will be obtained along with its intensity. And the procedure is to be repeated till we get all the lifetime. Thankfully, there are different softwares to do this analysis and the one I used is PALSfit.

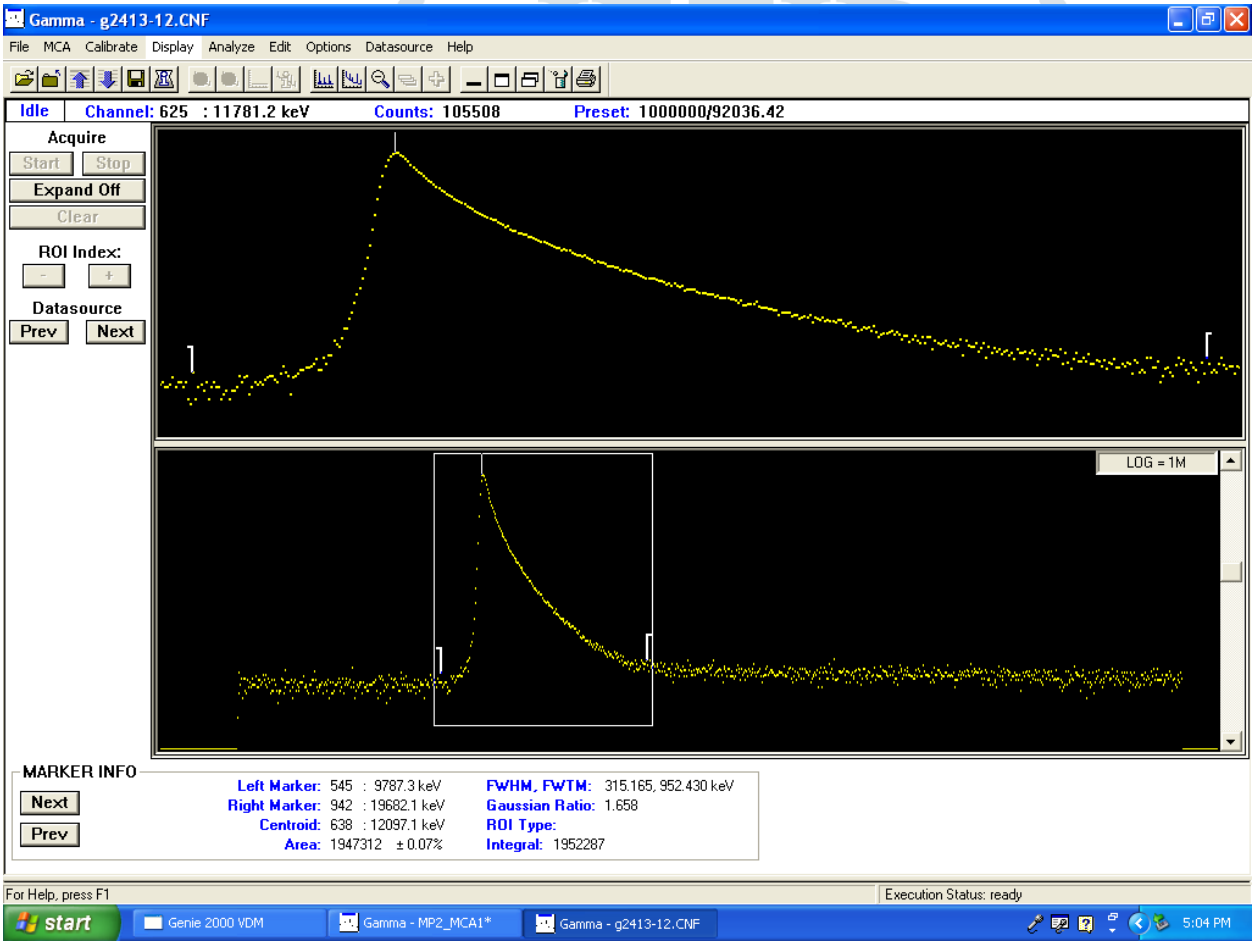

Figure2.7. Lifetime Spectrum

Source correction and Summation effect

There are fallacious detections due to positrons annihilating inside the source, scattering at the source-sample interfaces and annihilation at the nickel foil embedding the source. An equation for the no of positrons annihilating at the nickel foil is:

$I_{foil} = 0.324\ Z^{0.93}\ d^{3.45(z\text{^}-0.41)}$, where Z is the atomic no and d is the thickness of foil in mg/cm^2. The intensity of the back scattered positrons and those annihilating inside the source are found with the help of data analysis using PALSfit. The sample taken for source correction measurement is a pure perfectly single crystalline

substance, in our case it is well annealed Aluminium. These source corrections are to be removed by the PALSfit software from the data analysis spectrum of the samples.

Summation effect is another hindrance in measuring the lifetimes. The 1.276 MeV birth gamma ray may Compton scatter in such a way that a part of scattered photon may be of near 0.511 MeV energy and wrongly interpreted by the detectors as stop signal. Such an effect cannot be avoided and have to be accepted to the spectrum.

Doppler Broadening Measurements

Doppler broadening measurements are done using the HPGe detectors. The resolutions of the detectors are calculated using MCA channels and is mostly near 1.2keV at 0.511MeV. These detectors are operated at 77^0K with help of liquid nitrogen to prevent leakage of thermally charged carrier currents. The experiment can be done using one detector, but doing a coincidence Doppler broadening spectra aids in reducing the background readings.

Figure2.8. High Pure Germanium Detectors

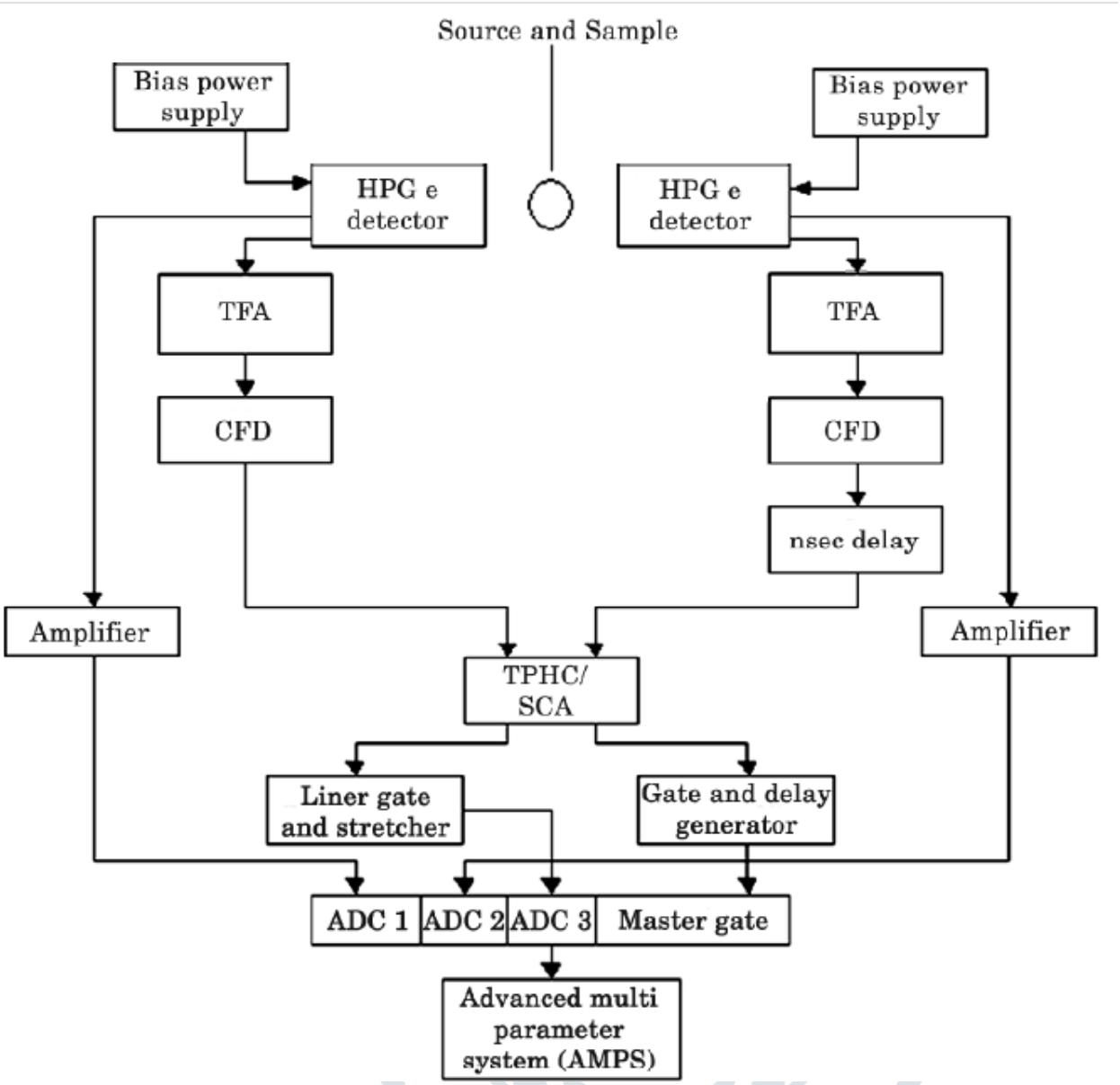

Figure2.9. Block diagram of the CDBS spectrum instruments

Data Analysis

Due to lack of appropriate mathematical functions, deducing information directly from the spectrum with the help of software is not possible. A good knowledge about the sample and the different probable defects is required. A good deal of info can be obtained about the evolution of defects due to doping, annealing etc.

The annihilation rays, being almost opposite, will be detected simultaneously by the two HPGe detectors. The output from these detectors will be split into two, similar to lifetime detection, so that one signal is used to plot in the CDBS spectrum while the other is used to strobe and check out the genuinity of the incoming signal.

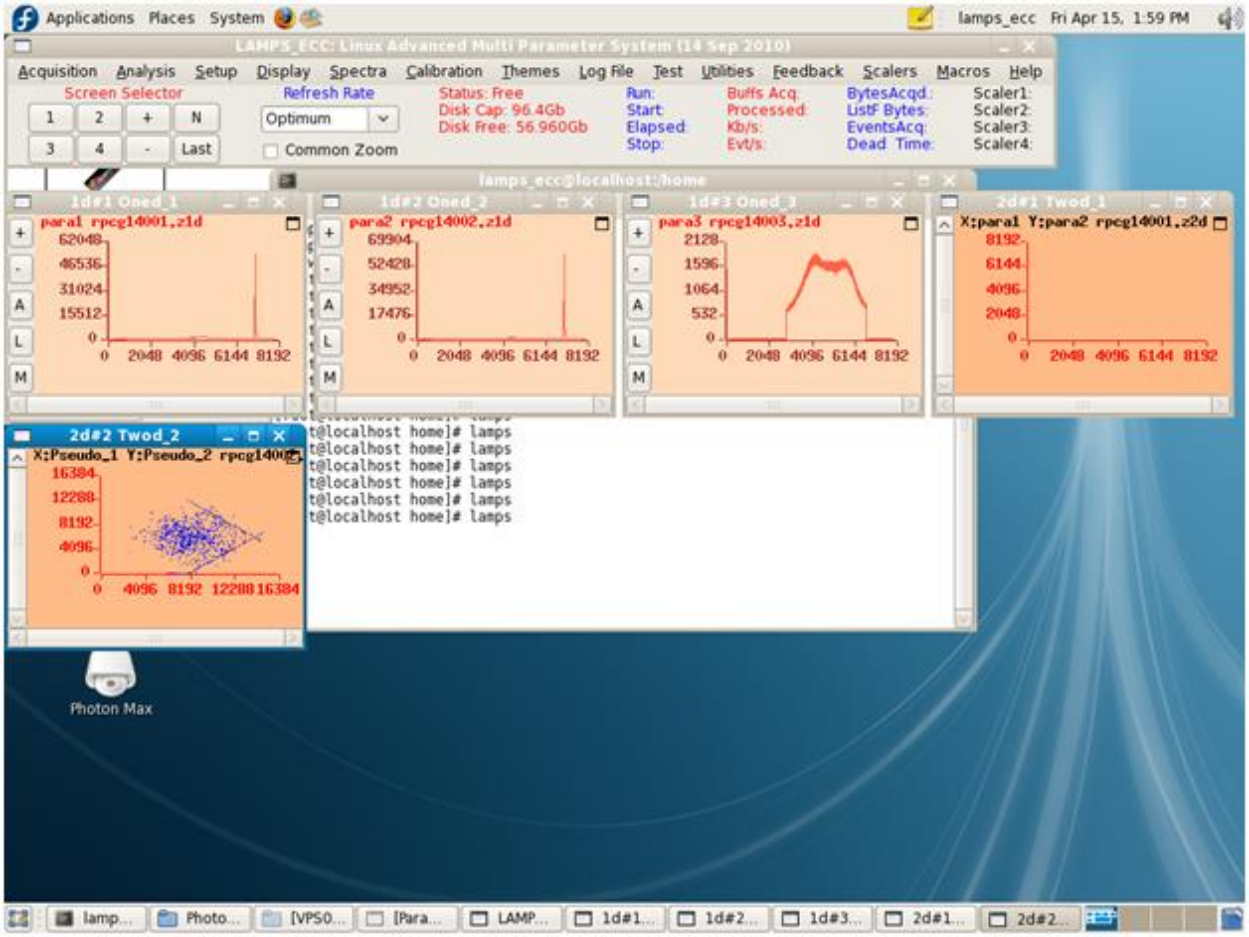

Figure2.10 Graphs plotted in CDBS spectrum

The produced graphs consists of two graphs denoting the energy spectrum from the two detectors with energy along the x-axis and counts along y, a two parameter spectrum with the total energy on the x-axis and the difference in energies of the simultaneous gamma rays in the y-axis and the total counts in the z-axis and two other graphs. Each energy spectrum has 8192 channels and hence the two parameter spectrum has 16384 channels.

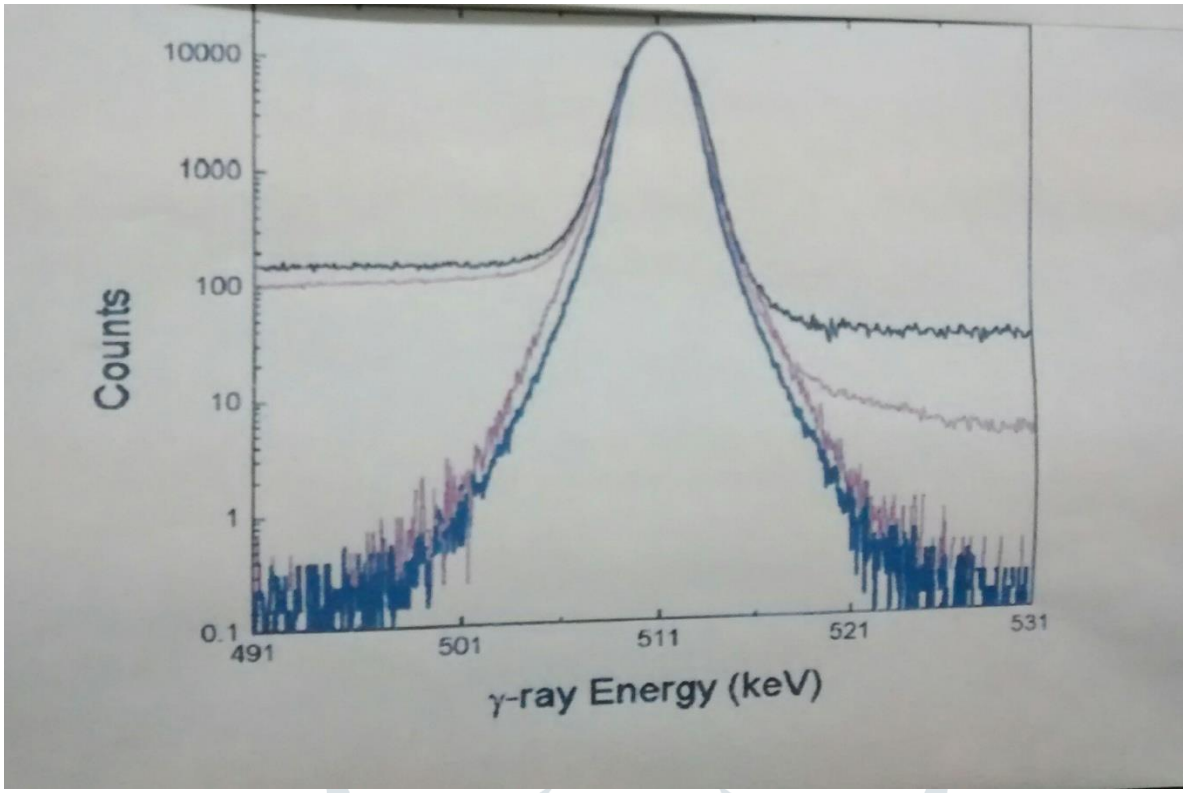

Figure2.11. Expected energy graph of one spectrum

The energy graph obtained from each detector is expected to be a symmetric Gaussian with an inverted parabola at the top. The peak of this graph corresponds to the 0.511MeV in the *x*-axis. Here, the central region, where the deviation (ΔE) from the 0.511MeV ray is low, is due to the valence electron. The Gaussian part of the curve, where ΔE varies largely, is due to the core electrons. The birth gamma ray will also be detected but will be mapped outside the CDBS spectra in the graph.

However, the birth gamma ray, may get Compton scattered and be reduced to the energy near the range of 0.511MeV. Due to Compton scattering, the gamma rays acquire a wide range of energies and this result in upward shift in the energy spectrum from the two detectors. This can be considered as unwanted background radiation, and the coincidence spectrum is taken mainly to overcome it. The 0.511MeV gamma rays may also get Compton scattered which further raise the counts of gamma rays that have less than 0.511MeV energy.

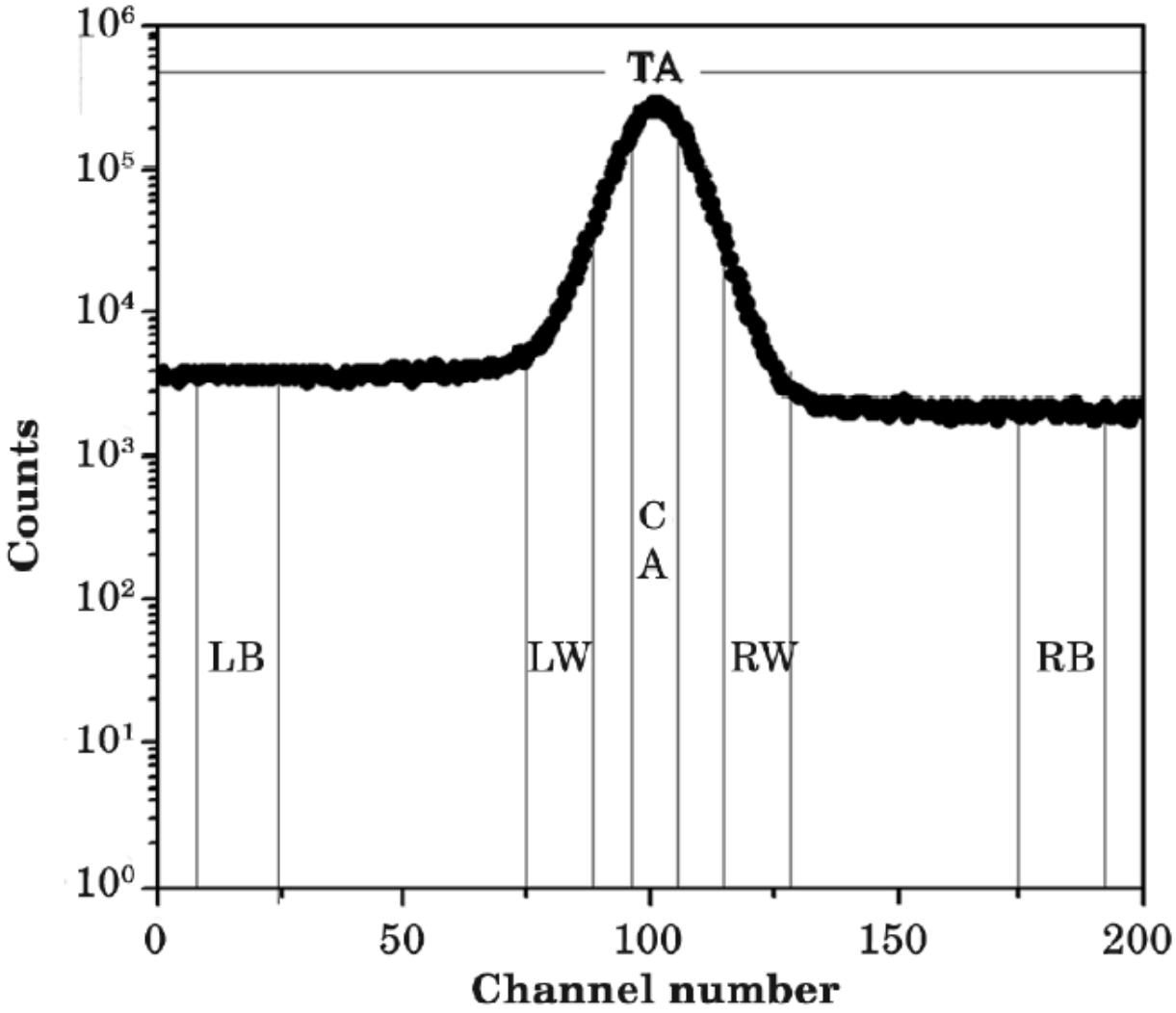

Figure2.12. Observed energy graph from one detector

The two parameter spectrum is of primary importance because it screens away the unwanted signal due to the birth gamma ray by coinciding the two signals from each detector. One detector records a signal as E_1 while the other records it as E_2. The total energy of simultaneous readings are plotted in the *x*-axis while *y*-axis plots the difference between these energies and the counts are plotted in the *z*-axis. Since total energy will be always near 1.022 MeV, the counts will be very high in that region and it thus forms a disk around the precise point. The readings of E_1 and E_2 can also be such that the total energy can be greater or lesser than 1.022MeV. Also, the prediction about which of the detectors the higher energy gamma ray may fall is not possible, it is random. Hence, sometimes E_1 can be greater than E_2 and vice versa. As a result there exists a mirror symmetry across the horizontal axis passing through point of total energy where the difference in energy of the two gamma rays are null. By producing a *y*-projection of this graph near the disk, with the center of disk as the center of the *y*-projection, valuable information regarding the momentum of core and valence electrons can be obtained.

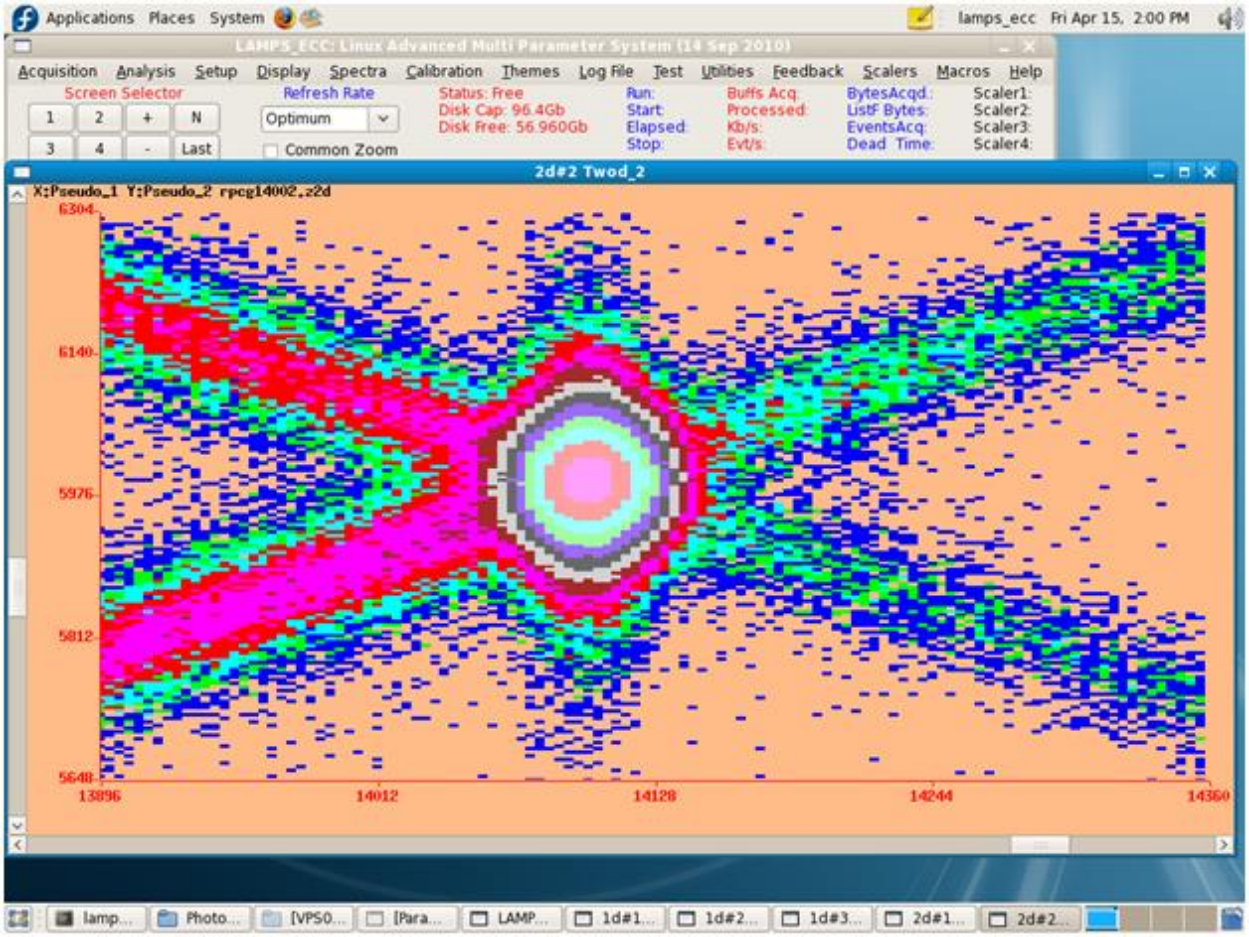

Figure2.13. Two Parameter CDBS spectrum

Chapter 3

RESULT AND DISCUSSION

1. **MGO FILES**

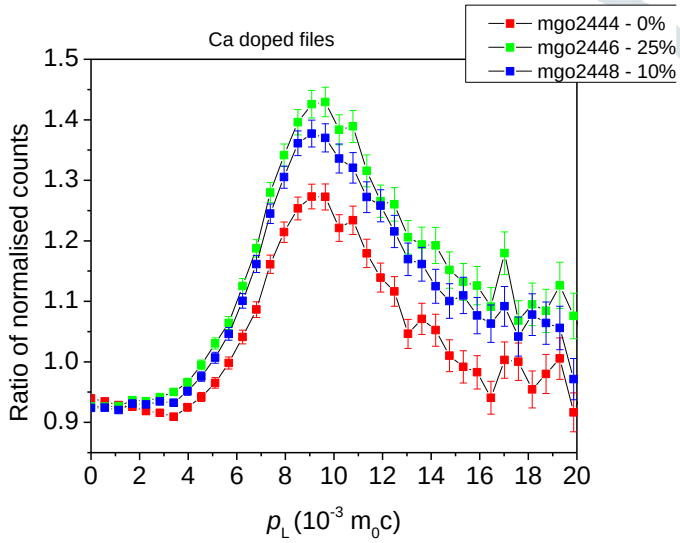

Figure3.1. Ratio of normalized counts versus electron momentum spectrum

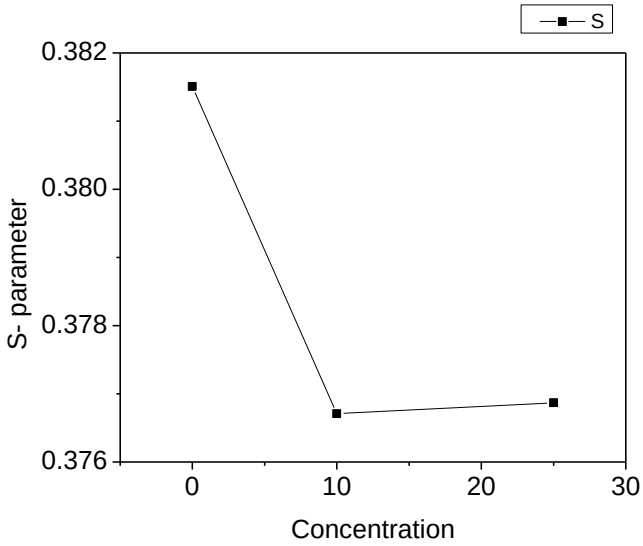

Figure3.2. S vs concentration

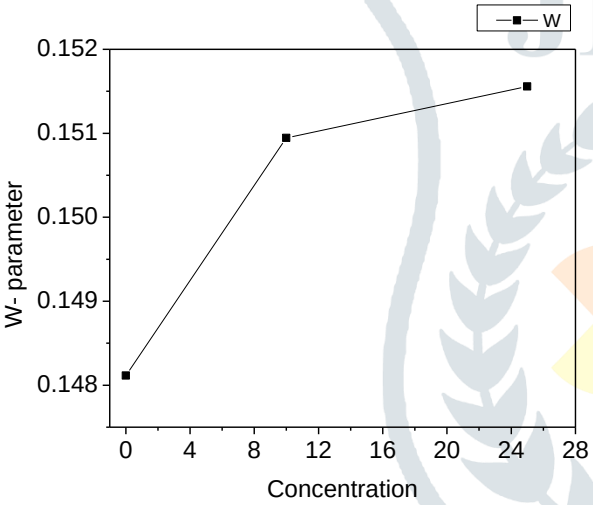

Figure3.3. W vs concentration

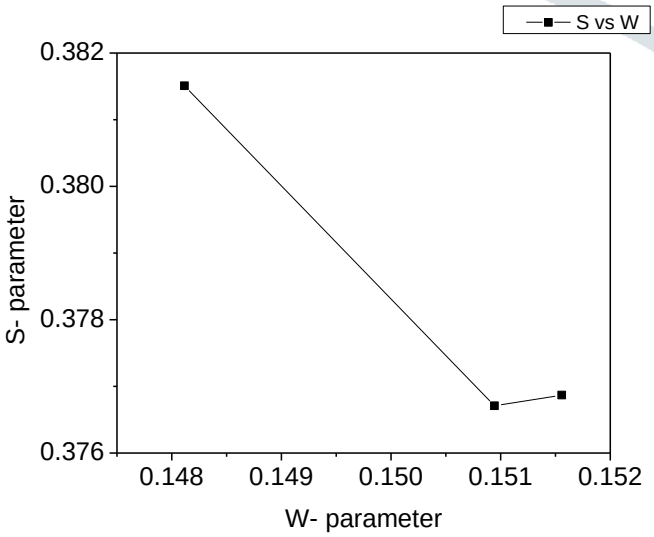

Figure3.4. S vs W parameters

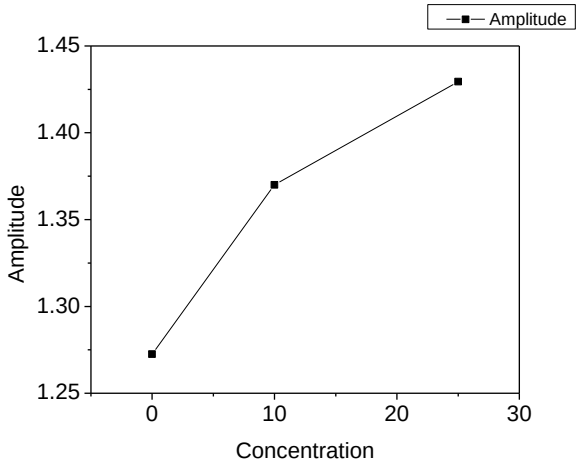

Figure3.5. Amplitude Vs Concentration

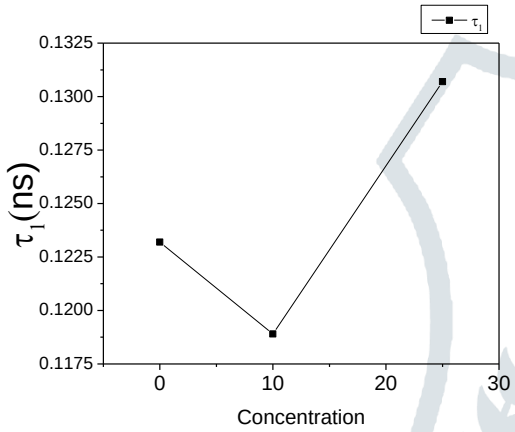

Figure3.6. bulk lifetime vs concentration

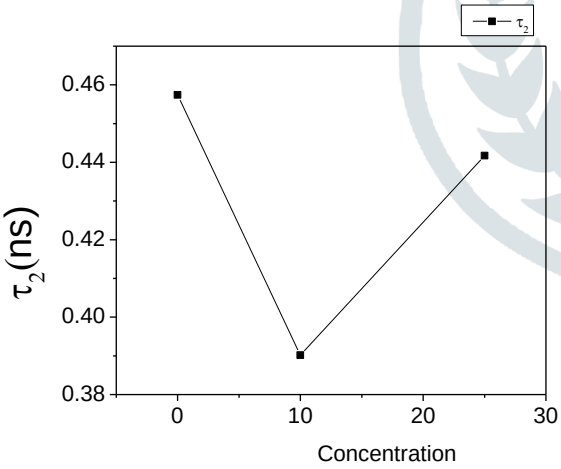

Figure3.7. defect lifetime vs concentration

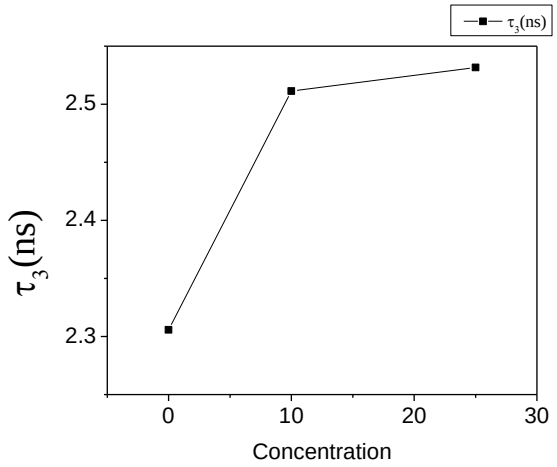

Figure3.8. Orthopositronium lifetime vs concentration

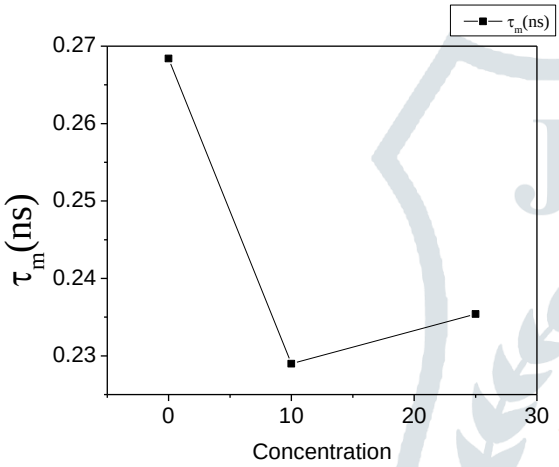

Figure3.9. Mean positron lifetime vs concentration

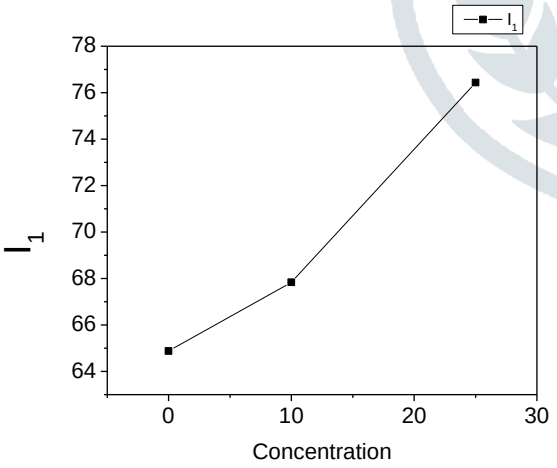

Figure3.10. Bulk positron Intensity vs concentration

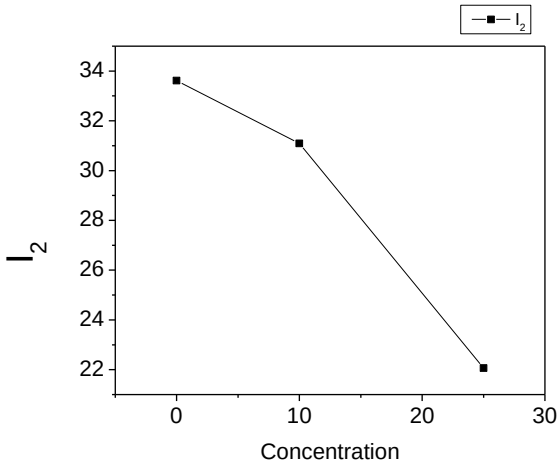

Figure3.11. Defect positron intensity vs concentration

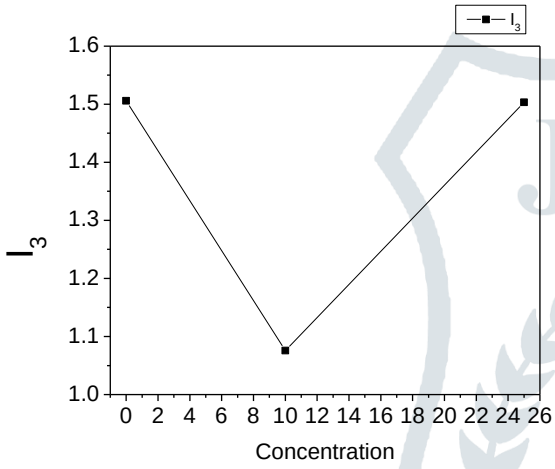

Figure3.12. Orthopositronium intensity vs concentration

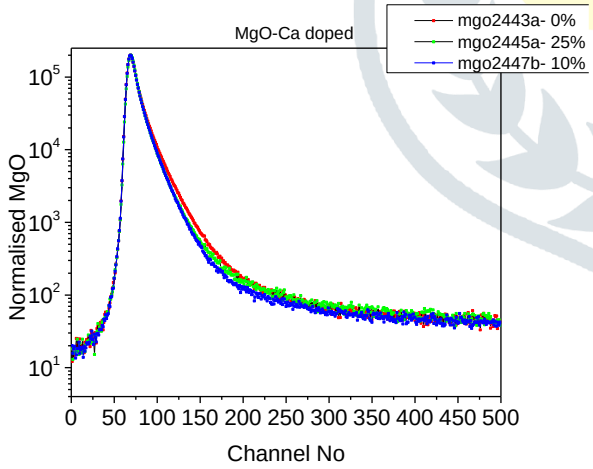

Figure3.13. Peak normalized graph of mgo

2. **MGF FILES – Post irradiated Magnesium Ferrite sample**

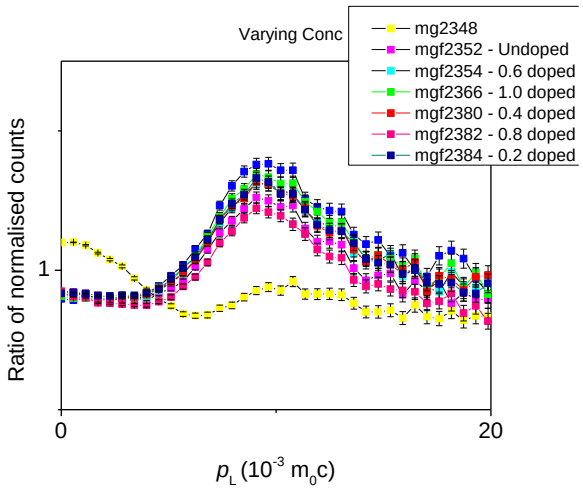

Figure3.14. Ratio of normalized counts versus electron momentum spectrum with varying concentration

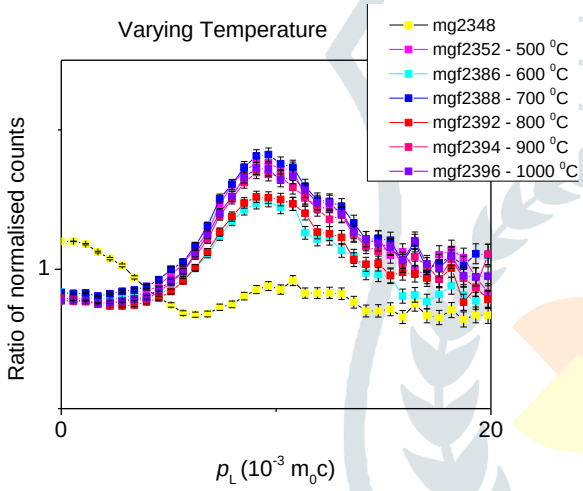

Figure3.15. Ratio of normalized counts versus electron momentum spectrum with varying temperature

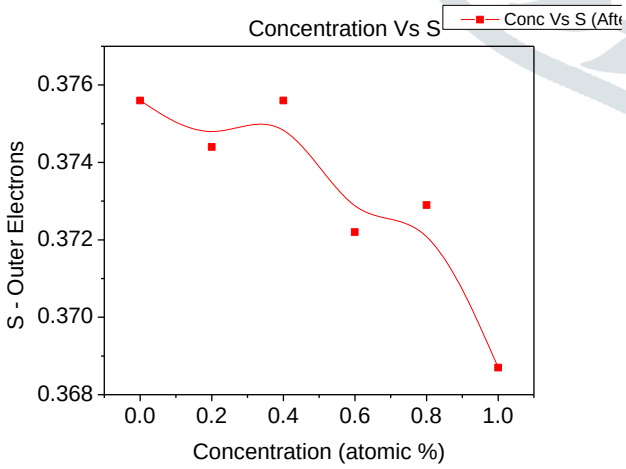

Figure3.16. S vs concentration

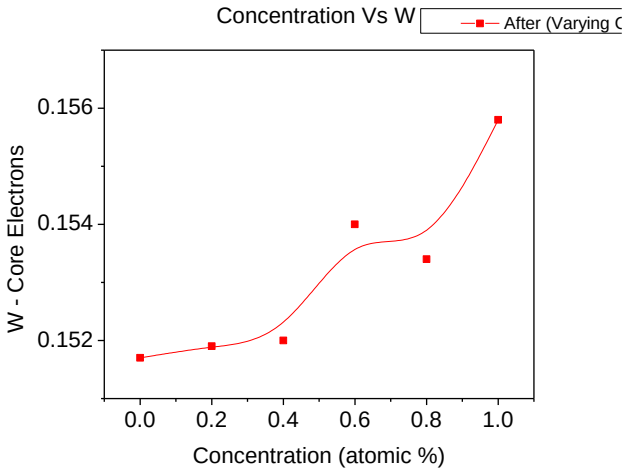

Figure3.17. W vs concentration

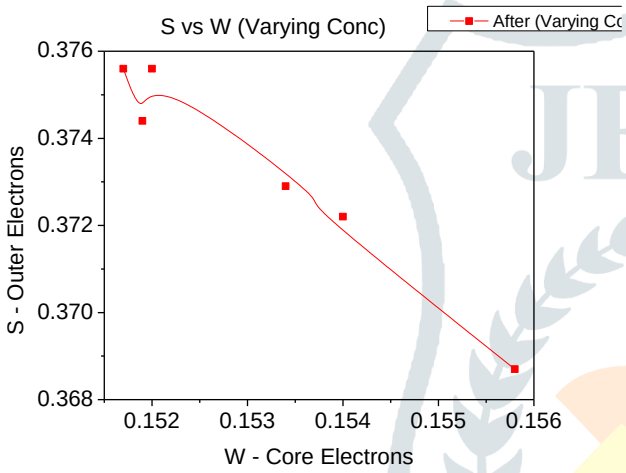

Figure3.18. S vs W parameters of varying concentration sample

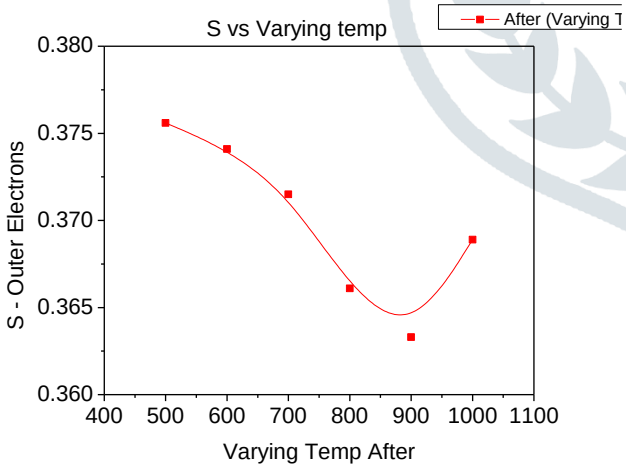

Figure3.19. S vs temperature

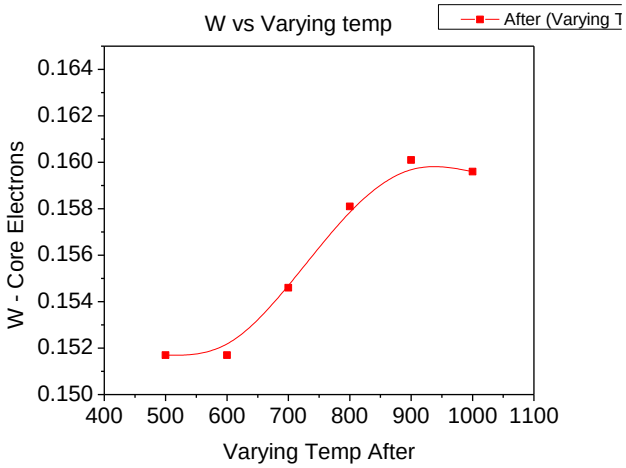

Figure3.20. W vs temperature

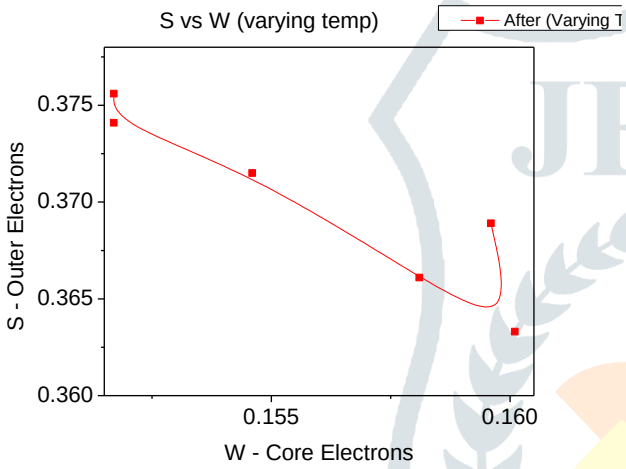

Figure3.21. S vs W spectrum of the varying temperature samples

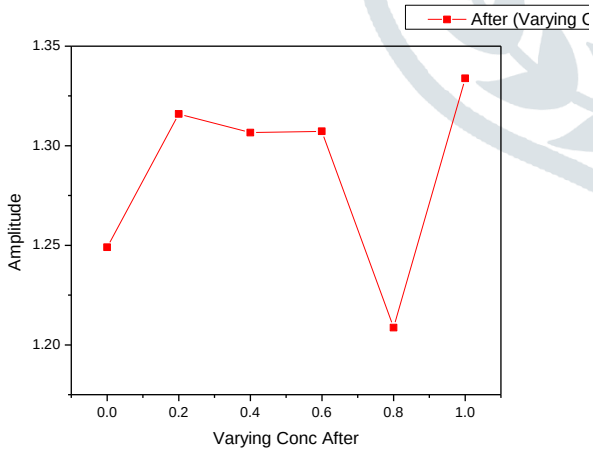

Figure3.22. Amplitude vs concentration

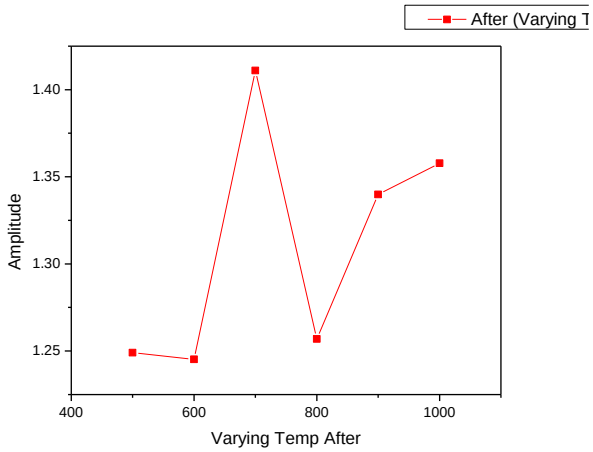

Figure3.23. Amplitude vs temperature

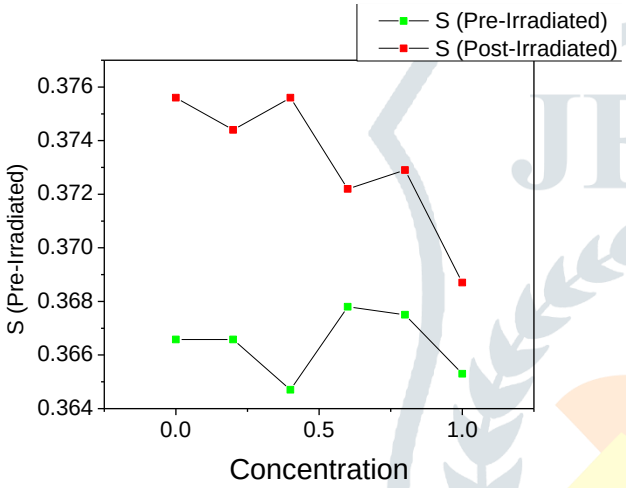

Figure3.24. Comparing S parameters with varying concentration of pre-irradiated and post-irradiated samples

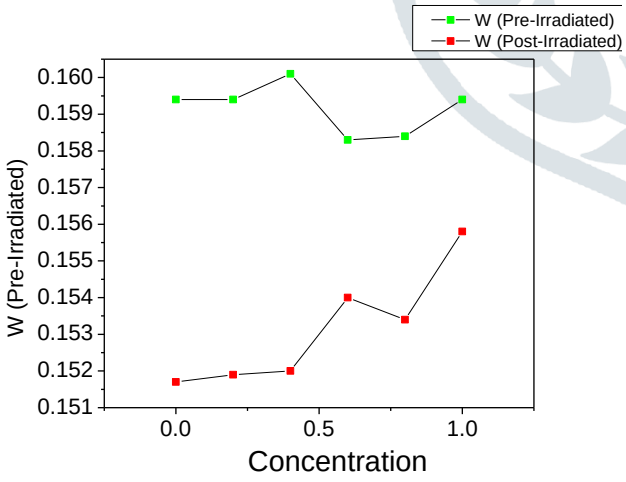

Figure3.25. Comparing W parameters with varying concentration of pre-irradiated and post-irradiated samples

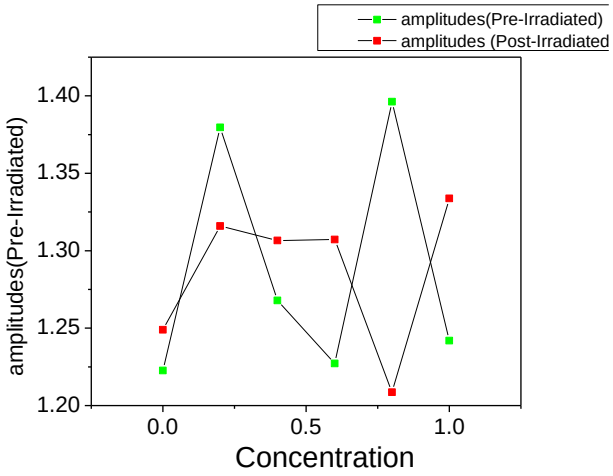

Figure3.26. Comparing amplitude with varying concentration of pre-irradiated and post-irradiated samples

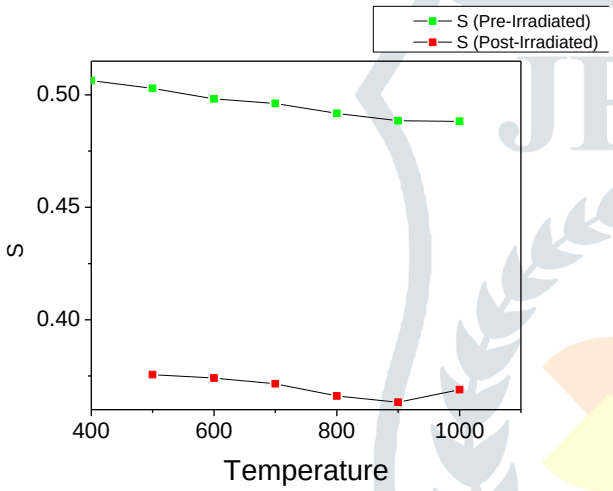

Figure3.27. Comparing S parameters with varying temperature of pre-irradiated and post-irradiated samples

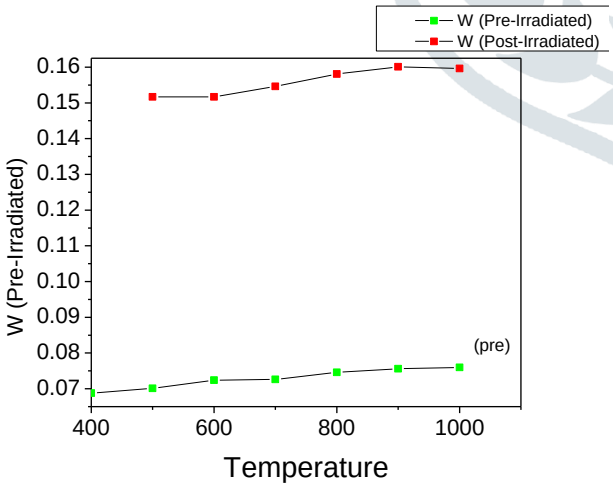

Figure3.28. Comparing W parameters with varying temperature of pre-irradiated and post-irradiated samples

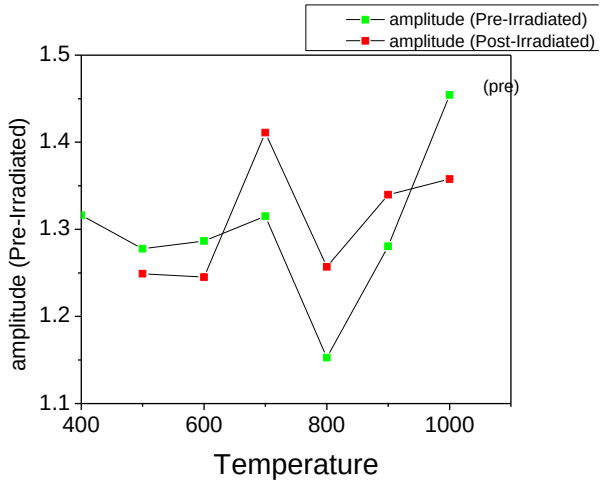

Figure3.29. Comparing amplitude with varying temperature of pre-irradiated and post-irradiated samples

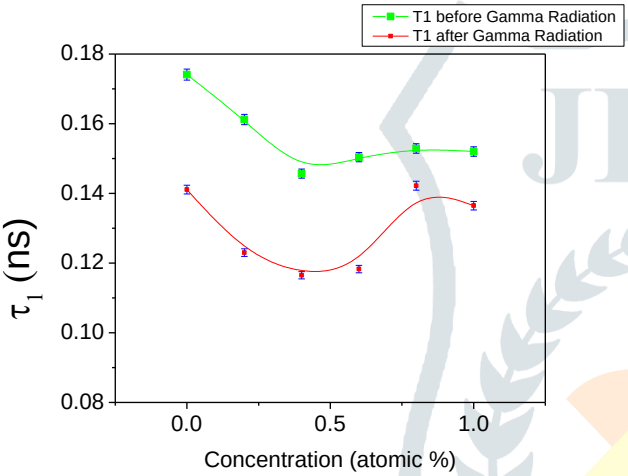

Figure3.30 Bulk lifetime merged with parapositronium component of positrons of samples with varying concentration

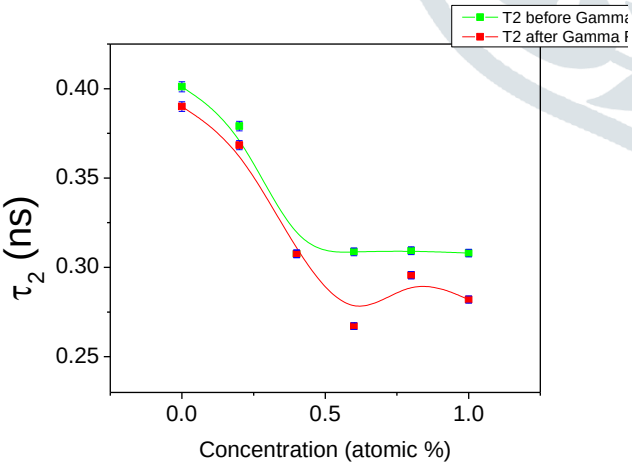

Figure3.31 Defect lifetime of positrons of samples with varying concentration

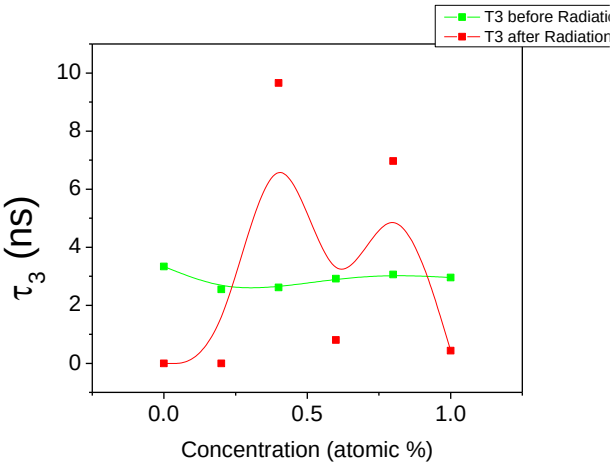

Figure3.32 Orthopositronium lifetime of positrons of samples with varying concentration

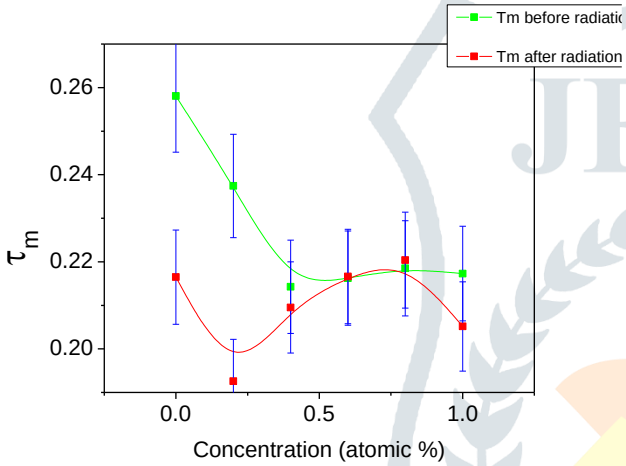

Figure3.33 Mean lifetime of positrons of samples with varying concentration

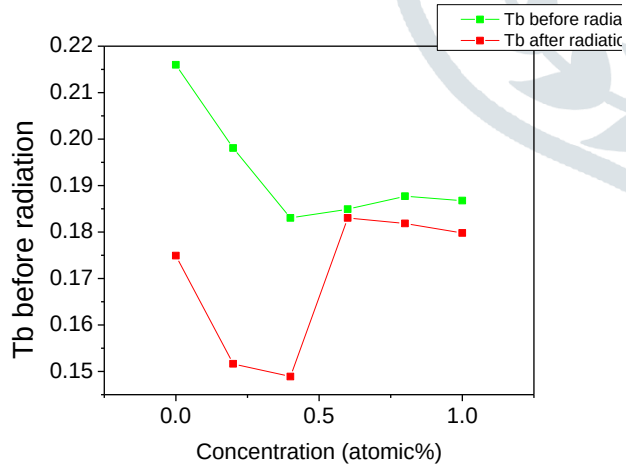

Figure3.34 Bulk lifetime of positrons of samples with varying concentration

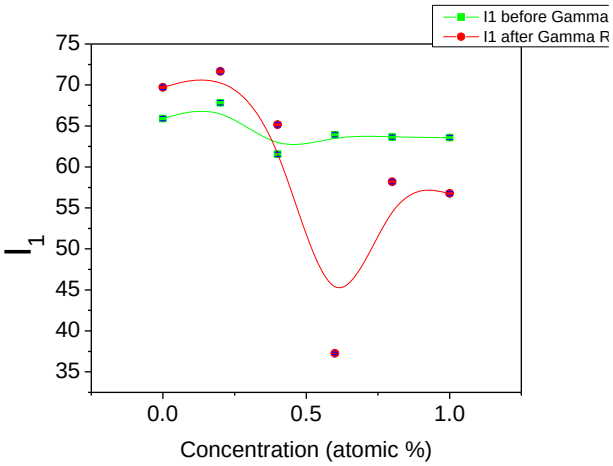

Figure3.35 Intensity of bulk positrons of samples with varying concentration

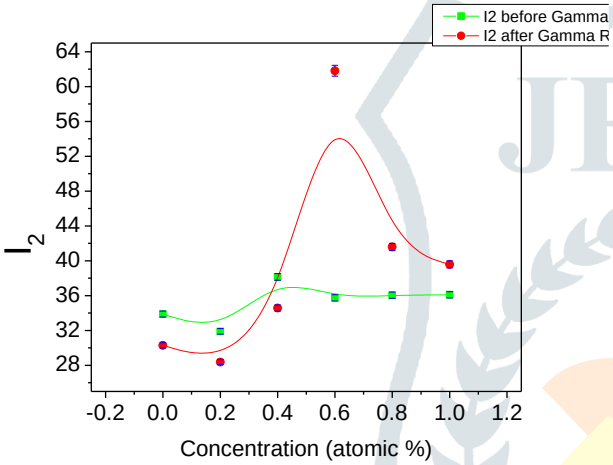

Figure3.36 Intensity of defect positrons of samples with varying concentration

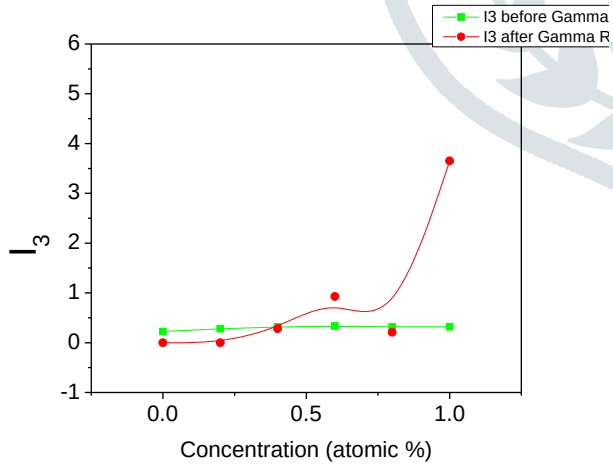

Figure3.37. Intensity of orthopositronium of samples with varying concentration

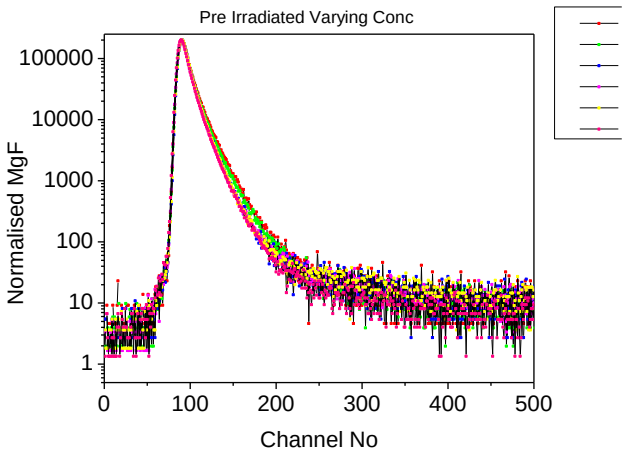

Figure3.38. Peak normalized spectrum of pre-irradiated mgo samples with varying concentration

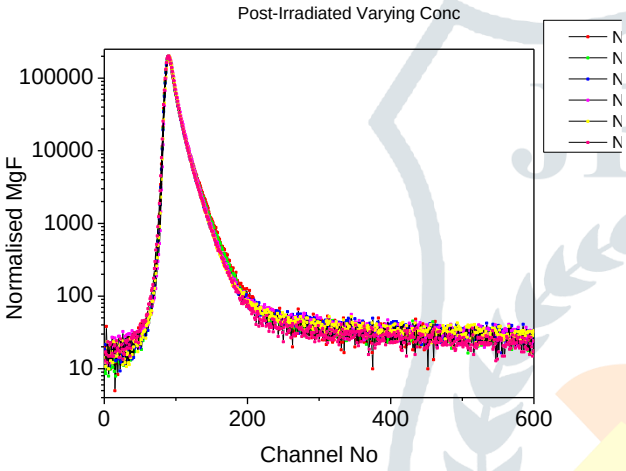

Figure3.39. Peak normalized spectrum of post-irradiated mgo samples with varying concentration

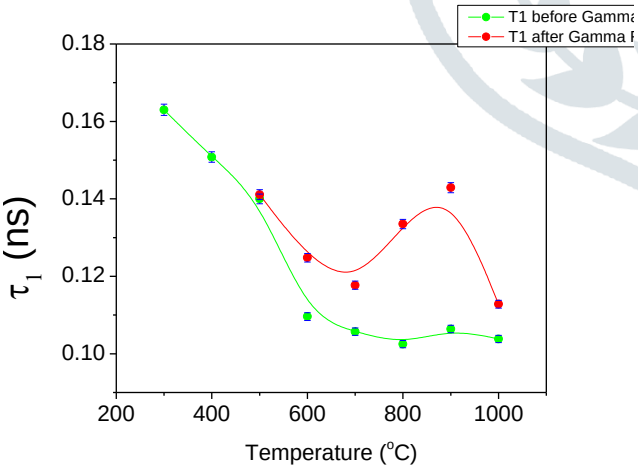

Figure3.40 Bulk lifetime merged with parapositronium component of positrons of samples with varying concentration

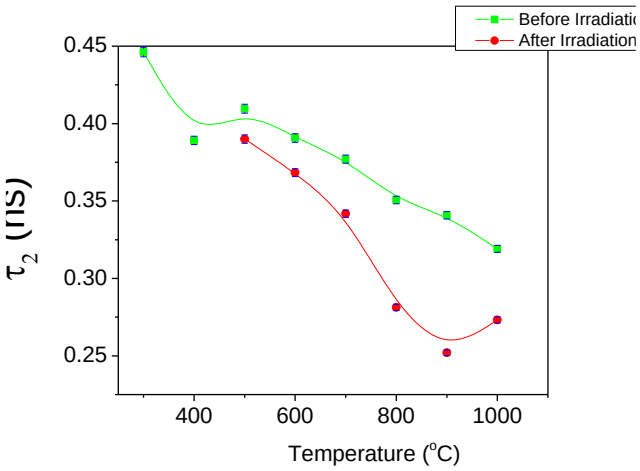

Figure3.41 Defect lifetime of positrons of samples with varying temperature

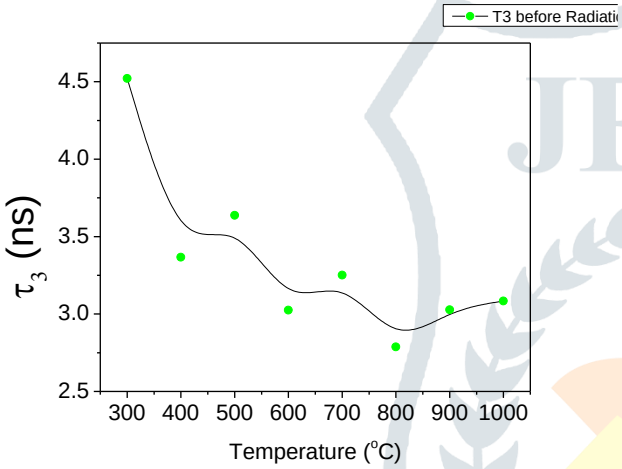

Figure3.42 Orthopositronium lifetime of samples with varying temperature

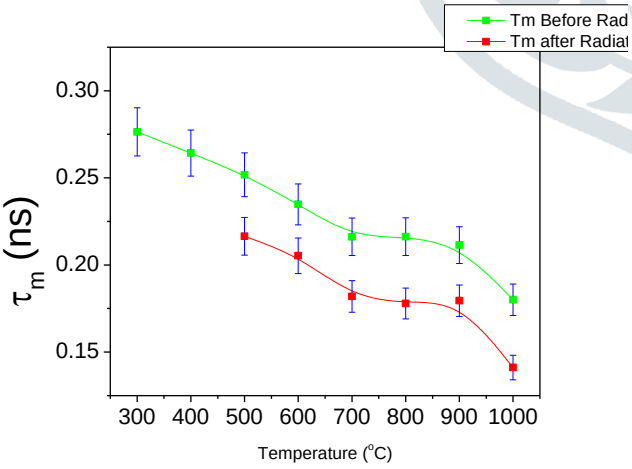

Figure3.43 mean lifetime of positrons of samples with varying temperature

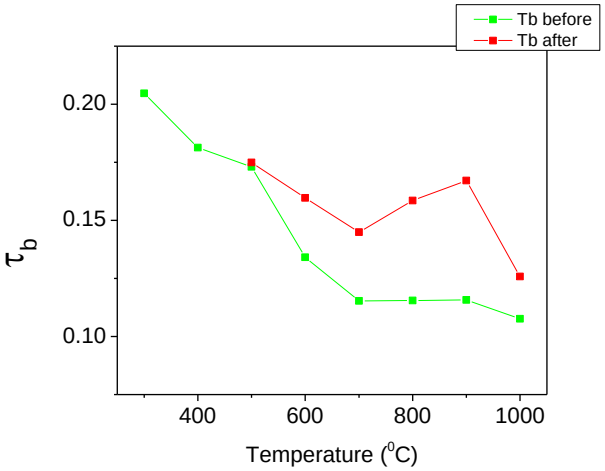

Figure3.44 Bulk lifetime of positrons of samples with varying temperature

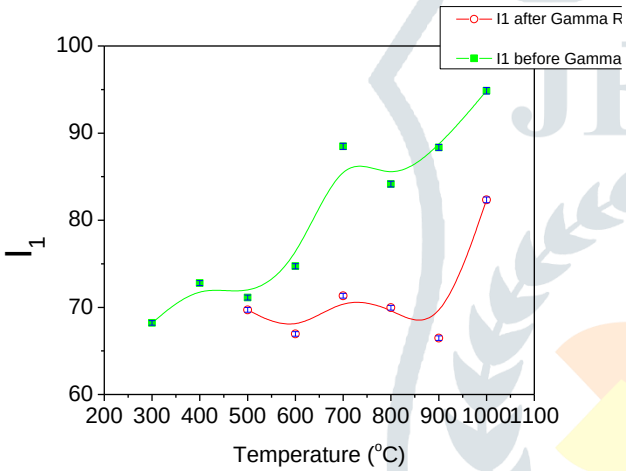

Figure3.45. Intensity of bulk positrons

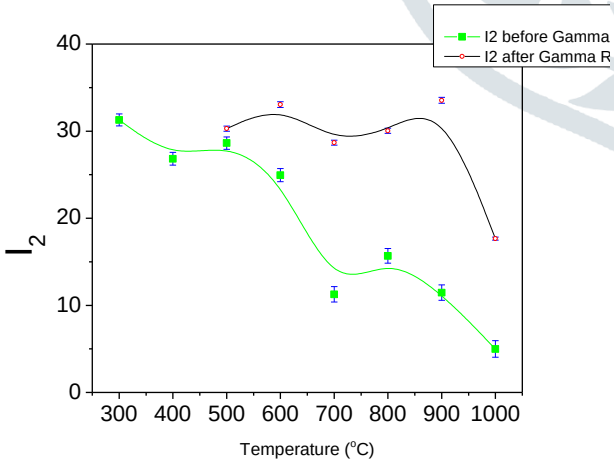

Figure3.46. Intensity of defect positrons

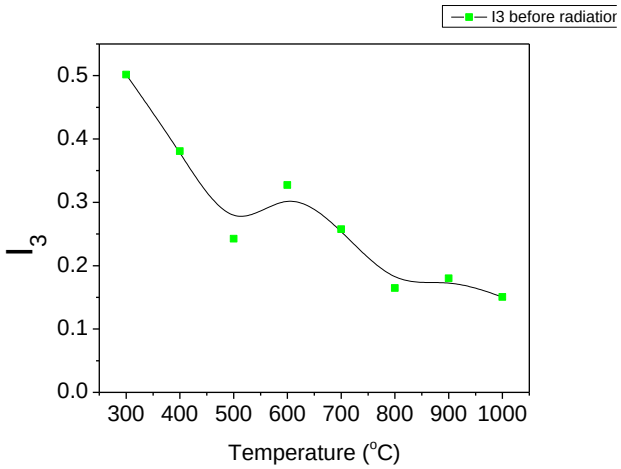

Figure3.47. Intensity of orthopositroniums

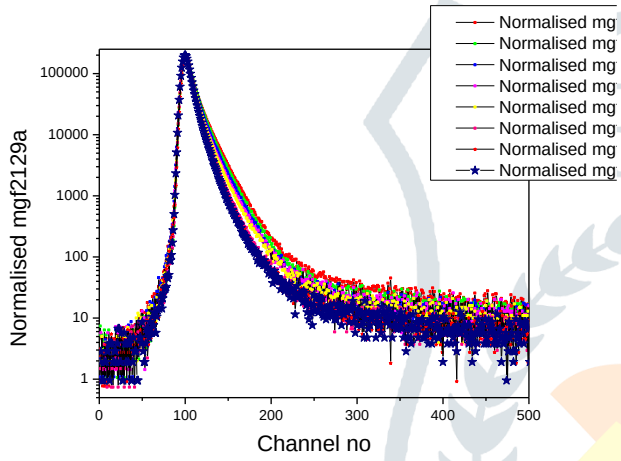

Figure3.48. Peak normalized spectrum of pre-irradiated mgo samples with varying Temperature

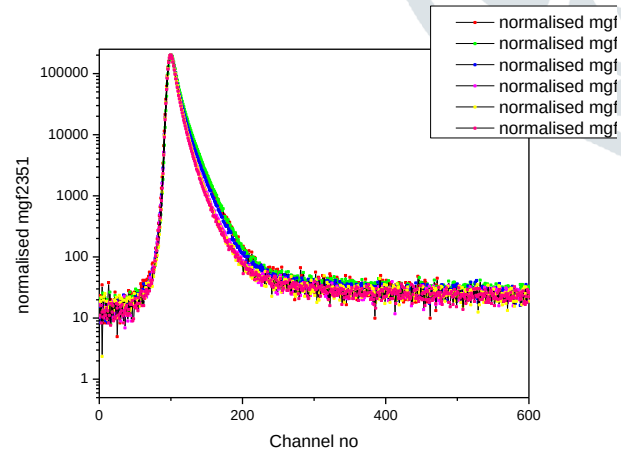

Figure3.49. Peak normalized spectrum of post-irradiated mgo samples with varying Temperature